Photophysical Properties of Fluorescent Polymers Containing 1,10-Phenanthroline-3,8-ylene and Diethinylenebenzene Units and Their Model Compounds: A Comparison to 2,2′-Bipyridine Analogues

U.-W. Grummt,[1,3] E. Birckner,[1] M. Al-Higari,[2] D. A. M. Egbe,[2] and E. Klemm[2]

Investigation of the absorption and emission spectra (stationary and time-resolved) of phenanthroline-based polymers shows that the enforcement of a cisoid geometry in the bipyridine unit of the main chain via an ethenylene bridge does not significantly change the spectral and the deactivation behaviour. In close analogy to similar polymers, containing bipyridine units, the conjugation length in these polymers does not exceed ca. two chromophore units. At low temperatures, the model compounds show an additional, bathochromically shifted, intense luminescence with an increased lifetime which can be interpreted as an excimer (or aggregate) fluorescence. In addition, broad, superimposed emission bands arising from various aggregated species are observed. The relative intensity of these bands depends on the temperature processing occurring during cooling. Intersystem crossing is an insignificant deactivation channel.

INTRODUCTION

Certain conjugated polyarenes have recently been the focus of considerable interest due to their potential, among other things, for serving as materials for electroluminescence devices [1] since they possess a high fluorescence efficiency and are technically processable. Furthermore, this class of polymers shows high second order non-linear susceptibilities [2,3]. In particular, high first order hyperpolarizabilities can be expected if hetero-aromatic systems which are able to form metal chelates are incorporated into the polymer [4].

From the viewpoint of basic rather than applied research, segmented conjugated polyarenes are useful objects for investigating energy migration along the polymer chain [5,6]. For instance, the antenna effect could be exploited in order to significantly enhance the sensitivity of a fluorescent chemosensor [7]. In particular, fluorescent rigid rod oligomers and their model compounds are excellent probes for studying molecular motions in viscous media via static and kinetic monotoring of the fluorescence anisotropy. An additional, interesting aspect is their potential use as molecular wires [8].

Ley and Schanze reported the first synthesis of a polymer containing 2,2′-bipyridylethynylene in the backbone. Metal complexes of this polymer as well as two model compounds were also included in this study [9]. In addition, these authors have also published photophysical

[1] Institut für Physikalische Chemie der Friedrich-Schiller Universität Jena, Lessingstrasse 10, D-07743 Jena, Germany.
[2] Institut für Organische und Makromolekulare Chemie der Friedrich-Schiller Universität Jena, Humboldtstrasse 10, D-07749 Jena, Germany.
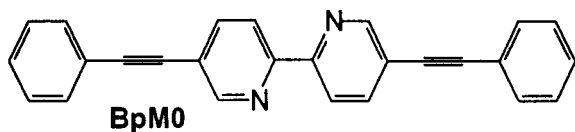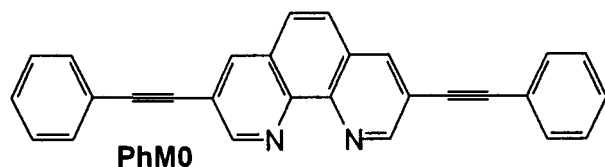[3] To whom correspondence should be addressed. Fax: +49-641 948302. E-mail: cug@uni-jena.de

data for a few compounds of this type. In a recent paper [10], we reported the absorption and emission spectra of new linear and angular conjugated polymers, oligomers and their model compounds all of which contain 2,2-bipyridine and diethinylene-benzene units in their backbone.

The current study has been initiated in order to answer the following questions: what effect does the replacement of the bipyridine moieties by phenanthroline have on the positions of the spectral transitions and on the conjugation length of the polymers? The most stable conformation of 2,2′ bipyridine is the transoid one. However, the rotational barrier is comparatively small (31 kJ/mol) and the difference of Gibbs free energy between the twisted cisoid and the planar transoid conformation is about 27 kJ/mol [11], which means that both forms are in an equilibrium with each other that can be readily established at room temperature. Does the restricted rotation of the pyridine moieties and thus their dipole moment perpendicular to the long molecular axis affect the deactivation behaviour of the excited state? For the unsubstituted model compound **PhM0** (first described in references [12] and [13]), intersystem crossing and a weak phosphorescence is observed which is absent in **BpM0** [14].

In addition, we addressed the question of whether or not alkoxy substitution prevents intersystem crossing due to an increase in the energy gap between the lowest $\pi\pi^*$ and $n\pi^*$ states by comparing bipyridine-containing model compounds and polymers containing alkoxy substituents of varying chain lengths with their phenanthroline-containing counterparts.

Absorption, fluorescence, and fluorescence excitation spectra as well as fluorescence decay curves were measured in various solvents at room temperature. In addition, the fluorescence quantum yields and lifetimes were determined. Luminescence investigations at 77 K should clarify the role of intersystem crossing in the deactivation of the excited state.

EXPERIMENTAL

Synthesis

Compounds **BpM8**, and **BpM18** were synthesized according to reference [10]. 1,4-Bis(2,2′-bipyridine-5′-ylethynyl)-2,5-didodecyloxybenzene, **BpM12**, was prepared from 5-bromo-2,2′-bipyridine and 1,4-diethynyl-2,5-didodecyloxybenzene according to the procedure given in reference [10], m.p. 104–106°C. Analysis: $C_{66}H_{90}N_4O_2$ (914.46); calculated C 81.60, H 9.33, N 5.76; found: C 81.40 H 9.62 N 5.66%.
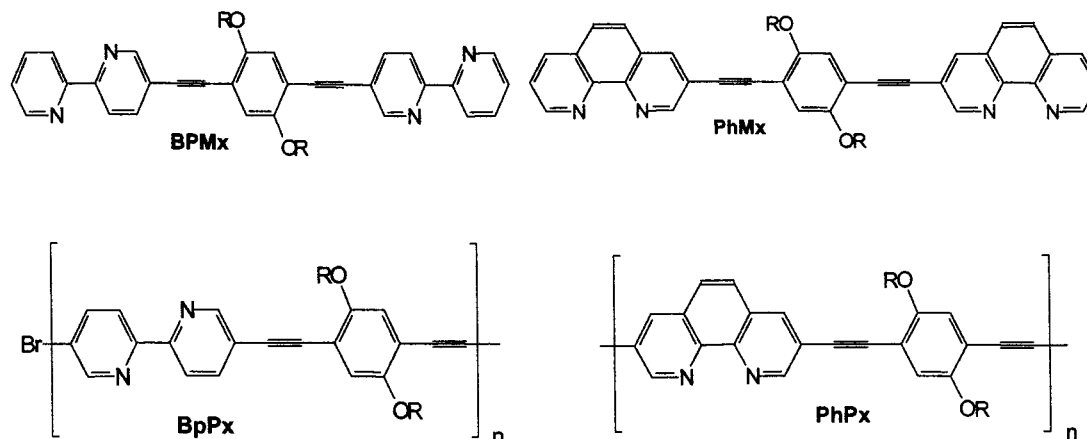
The preparation and characterization of the bipyridine containing polymers **BpP8** (R = C_8H_{17}), **BpP18** (R = $C_{18}H_{37}$) and their model compounds are described in reference [15]. The polymer **BpP12** (R = $C_{12}H_{25}$) was prepared in the same way. The number-average molecular weight M_n was determined by vapour pressure osmometry; M_n of the polymers is in the range of 11,000 to 13,000 g mol^{-1}, which corresponds to a degree of polymerization DP ≈ 15.

The preparation of compounds **PhM12** and **PhM18** is to be found in ref [12]. 1,4-Bis(1,10-phenanthroline-3-ylethynyl)-2,5-dioctyloxybenzene, **PhM8**, was similarly prepared from 3-bromo-1,10-phenanthroline and 1,4-diethynyl-2,5-dioctyloxy benzene, m.p. 119–121°C. Analysis: $C_{50}H_{50}N_4O_2$ (701.95), calculated C 81.26, H 6.82, N 7.59; found: C 80.91 H 7.12 N 7.06%.

The synthesis and characterization of the poly(3,8-(1′,4′-diethynylene-2′,5′-dialkoxyphenylene)-1,10-phenanthroline), **PhP12** (R = $C_{12}H_{25}$), and **PhP18** (R = $C_{18}H_{37}$) has been described in reference [12]. Polymer **PhP8** (R = C_8H_{17}) was prepared in the same way. The M_n was again determined by vapour pressure osmometry and is in the range of 7,000 to 9,000 g mol^{-1} which corresponds to 8<DP<9.

Instrumentation

Molar absorptivities were determined in CHCl$_3$ and/or 1,4-dioxane (HPLC quality; Baker) on a Perkin Elmer UV/VIS-NIR Spectrometer Lambda 19. Spectroscopic grade solvents (UVASOL; Merck) were used for all other spectroscopic investigations. Absorption spectra were recorded at room temperature on a LAMBDA 16 spectrophotometer (Perkin Elmer). Fluorescence and phospho-

PhM0

BpM0

Scheme 1.

Scheme 2.

R		bipyridyls	phenanthrolines
C_8H_{17}	model	**BpM8**	**PhM8**
	polymer	**BpP8**	**PhP8**
$C_{12}H_{25}$	model	**BpM12**	**PhM2**
	polymer	**BpP12**	**PhP12**
$C_{18}H_{37}$	model	**BpM18**	**PhM18**
	polymer	**BpP18**	**PhP18**

Bp and **Ph** stand for bipyridine and phenanthroline, respectively, **M** and **P** for model and polymer, the succeeding numbers designate the length of the alkyl substituents

Scheme 2.

rescence emission and excitation spectra were measured using a LS50B luminescence spectrometer (Perkin Elmer). Emission spectra were always recorded with excitation occuring at the longest wavelength absorption maximum. Fluorescence excitation spectra were measured at the emission maximum. The spectral slit widths of both the emission and excitation monochromators were set to 4 nm for all measurements. Low temperature experiments recorded at 77 K used the low temperature accessory of the LS50B spectrometer and were performed with samples that had been placed in fused synthetic silica tubes of 2 mm inner diameter. Fluorescence quantum yields were calculated relative to quinine sulphate (purum; FLUKA) in 0.1 NH_2SO_4 (pro analysi; Laborchemie Apolda) used as a standard (ϕ_f = 0.55) [16]. The absorbance at the excitation wavelength was kept below 0.05 for the samples and the reference. The kinetics of fluorescence was investigated with a CD900 time correlating single photon counting spectrometer (Edinburgh Instruments). The excitation source was a hydrogen filled nanosecond flashlamp which yielded an instrument response pulse of 1.3 ns FWHM. Polarizers with a vertical orientation on the excitation side and a 55° (magic angle) orientation on the emission side were used to avoid polarization effects. The kinetics of fluorescence was recorded at the emission maxima under excitation at the longest wavelength absorption maxima. The spectral slit width was 18 nm. Decay curves were accumulated until 10^4 counts in the maximum with at least 10^3 occupied channels. The channel width corresponded to 13 ps.

In order to calculate the fluorescence lifetime, the LEVEL 1 (up to 4 exponentials) and LEVEL 2 (Distribution Analysis) packages implemented in the Edinburgh Instruments software were used. (The analysis makes use of the iterative reconvolution technique and the Marquardt fitting algorithm.) Plots of weighted residuals and of the autocorrelation function and values of reduced residuals χ^2 were used to judge the quality of the fit. χ^2

values larger than 1.3 were not accepted. The fluorescence kinetics of the model compounds measured under magic angle is, without execption, singly exponential and is independent of the emission wavelength. The fluorescence kinetics of the polymers (magic angle) shows deviations from first order decay. The mean lifetimes were therefore calculated; see Table I, footnote *b*.

RESULTS AND DISCUSSION

Figure 1 shows the absorption and fluorescence spectra of the model compounds **BpM18** and **PhM18** in cyclohexane (CH). The shapes of the longest wavelength absorption bands resemble each other very closely for both compounds. The absorption maximum of the phenanthroline derivative is bathochromically shifted by a few nanometers. The molar absorptivities measured in chloroform differ by 20%. This, however, lies within the 10% overlap of the error intervals. Significant differences between both spectra can be seen in the short wavelength uv region. The 330 nm band is essentially caused by the alkoxy substitution and is less intense for **PhM18** as compared to **BpM18**. The increased absorption near 280 nm can be assigned to local transitions of the phenanthroline subchromophor, (phenanthroline/heptane: $\lambda_a = 263$ nm ($\epsilon = 26500$), $\lambda_a = 231$ nm ($\epsilon = 54000$); bipyridyl/nonpolar solvent: $\lambda_a = 247$ nm ($\epsilon = 17000$)) [17].

The fluorescence spectra of both compounds are surprisingly similar. The vibrational structure of the fluorescence spectrum is more pronounced as compared to the absorption spectrum; an observance that is typical for this class of compounds and which indicates that the S_1 state has a more rigid structure.

Figure 2 shows the absorption and fluorescence spectra of the model compounds containing bipyridine and phenanthroline as well as all polymers that had been substituted by $OC_{12}H_{25}$. The measurements were performed in dioxane at room temperature. The absorption spectra of the model compounds in dioxane closely resemble those of the compounds containing long-chain substituents in CH. The fluorescence spectra are, however, bathochromically shifted and clearly less structured.

Both polymers absorb at slightly longer wavelengths than their model counterparts. The phenanthroline absorption band of the polymer which occurs at 280 nm remains unchanged but decreases in intensity as does the 330 nm band. The difference between the bipyridine and the phenanthroline compound is astonishingly small not only in the case of the model compounds but also for the polymers.

Similar results were obtained upon comparing the compounds with $R = C_{12}H_{37}$ and $R = C_8H_{17}$. Table I shows the spectral and photophysical data measured in dioxane at room temperature of the polymers and the model compounds. The properties of the model com-

Table I. Absorption Maxima (λ_a) and Extinction Coefficients (ϵ), Fluorescence Maxima (λ_f), Stokes Shifts ($1/\lambda_a - 1/\lambda_f$), Quantum Yields ($\Phi_f$), Lifetimes τ and Rate Constants of Fluorescence ($k_f = \Phi_f/\tau$), and Radiationless Deactivation Rates ($k_{nr} = (1 - \Phi_f)/\tau$) in Dioxane at Room Temperature

Code	R	λ_a (nm)	ϵ ($M^{-1} cm^{-1}$)[a]	λ_f (nm)	$\Delta\nu_{af}$ (cm^{-1})	Φ_f	τ (ns)[b]	k_f (ns^{-1})[b]	k_{nr} (ns^{-1})[b]
BpM8	OC_8H_{17}	385	49000	431	2770	0.97	1.31	0.74	0.023
PhM8		392		436	2570	0.82	1.26	0.65	0.14
BpM12	$OC_{12}H_{25}$	385	47000	431	2770	0.96	1.33	0.72	0.030
PhM12		390		432	2440	1	1.29	0.78	0
BpM18	$OC_{18}H_{37}$	385	48000	432	2830	0.86	1.31	0.66	0.11
PhM18	$OC_{18}H_{37}$	390	40000	433	2550	0.99	1.32	0.75	0.008
BpP8	OC_8H_{17}	415	33000	456	2170	0.67	0.64	1.05	0.52
PhP8[c]	OC_8H_{17}	411		452	2210	0.70	—	—	—
BpP12	$OC_{12}H_{25}$	409	40000	453	2370	0.74	0.87	0.85	0.30
PhP12	$OC_{12}H_{25}$	405		453	2620	0.77	0.84	0.92	0.27
BpP18	$OC_{18}H_{37}$	410	40000	452	2270	0.56	0.70	0.80	0.63
PhP18	$OC_{18}H_{37}$	403		450	2590	0.68	0.87	0.79	0.37

[a] Solvent chloroform; this solvent was used for the determination of molar absorptivities ϵ because of the good solubility of all model compounds and polymers. Molar absorptivities of the model compounds are the same in chloroform, dioxane (and toluene) within an error interval of 10 %. Larger differences between chloroform and dioxane as solvents are observed for some of the polymers due to poor solubility in dioxane.

[b] τ, k_f, and k_{nr} for the polymers are weighted means from biexponential fits: $\langle\tau\rangle = 100/(\varphi_1/\tau_1 + \varphi_2/\tau_2)$ (for φ_1 and τ_1 see Table II), $k_f = \Phi_f/\langle\tau\rangle$, $k_{nr} = (1 - \Phi_f)/\langle\tau\rangle$.

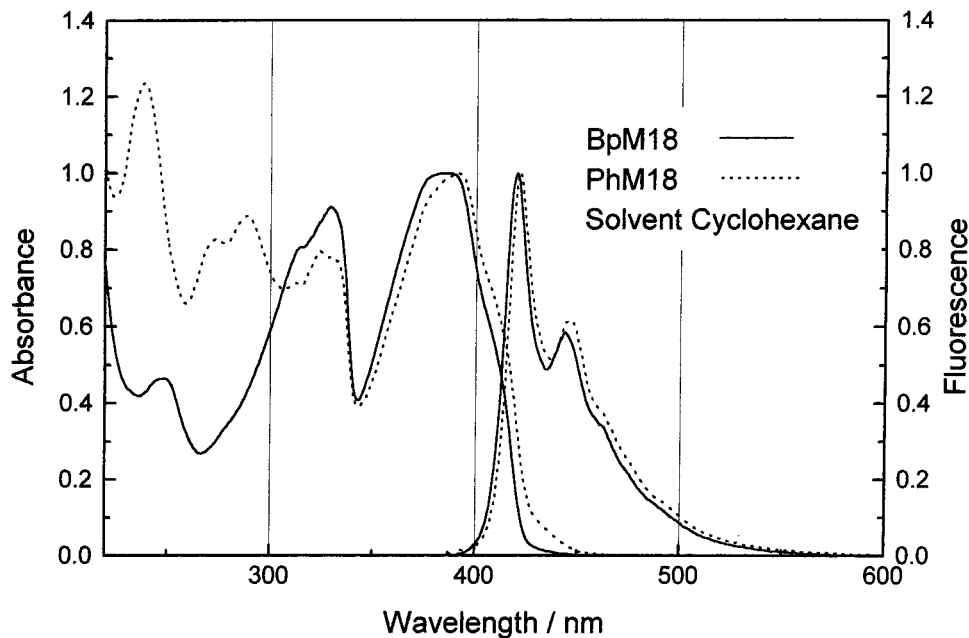[c] Data for PhP8 were obtained from toluene solutions.

Fig. 1. Absorption and fluorescence spectra of **BpM18** and **PhM18** in cyclohexane at room temperature.

pounds are again very similar to each other. The fluorescence quantum yields and the lifetimes vary merely within the error range ($\phi_f = 0.9 \pm 0.1$; $\tau = (1.3 \pm 0.05)$ ns). In addition, the polymer data do not differ much from each other. The decrease in the fluorescence quantum yield by roughly 20% indicates the presence of an additional deactivation channel which is probably quenching enhanced by energy migration.

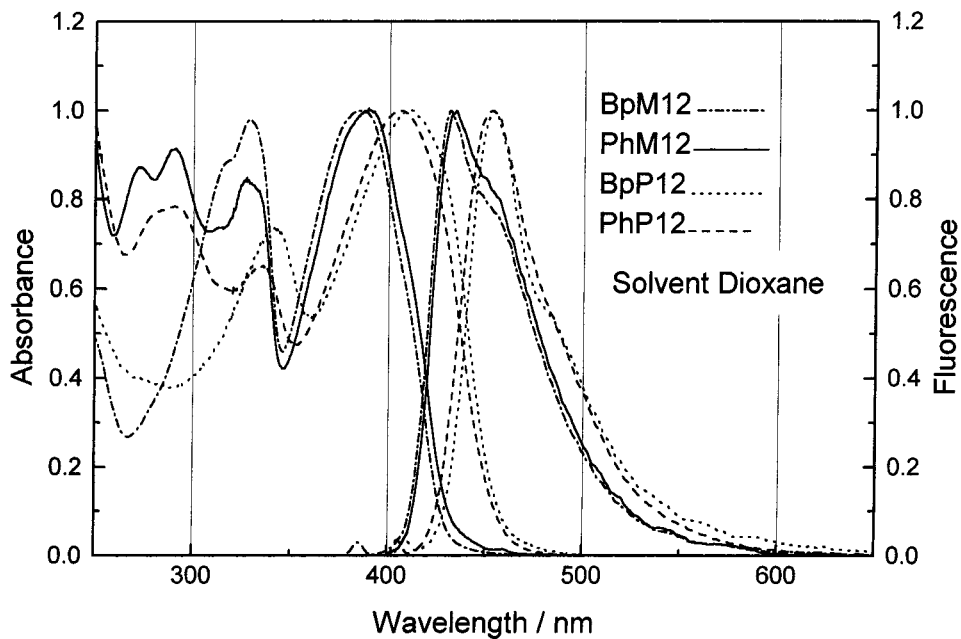In contrast to the monomer model compounds, the polymers do not exhibit a singly exponential fluorescence

Fig. 2. Absorption and fluorescence spectra of related models (**BpM12, PhM12**) and polymers (**BpP12, PhP12**) in dioxane at room temperature.
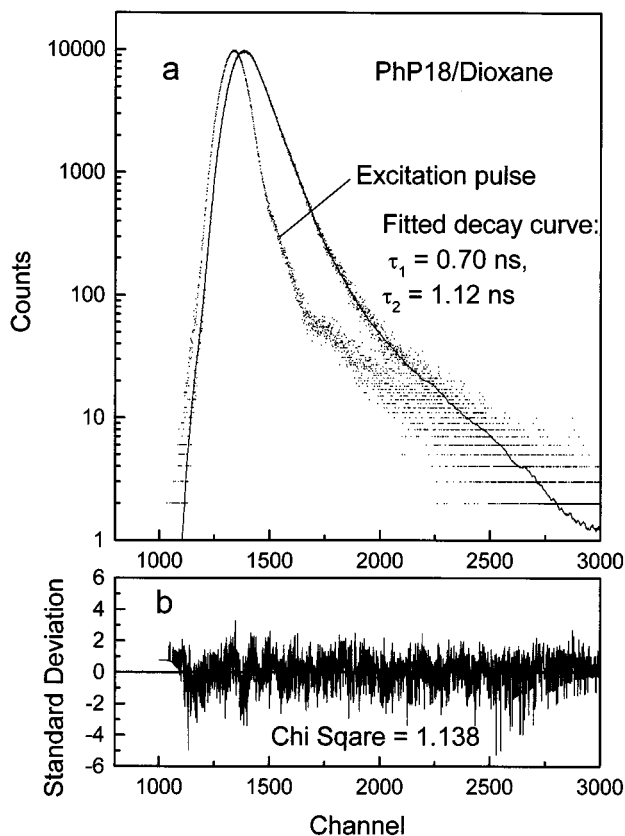
Fig. 3. (a) Excitation pulse and measured and calculated fluorescence decay and (b) residuals (Std Dev) of **PhP18** in dioxane at room temperature; channel width = 13 ps.

decay. The experimental decay curves are well represented by two exponentials with the larger decay time agreeing well with that of the models (cf. Fig. 3, for example). The results of the biexponential fits are given in Table II.

Systematic fluorescence kinetics investigations on poly(aryleneethynylene)s in solution have, as to date, not been reported in the literature. We therefore measured

Table II. Polymers in Dioxane at Room Temperature[a]

	τ_1 (φ_1)	τ_2 (φ_2)	χ^2	DW
BpP8	0.58 ns (78%)	0.97 ns (22%)	1.14	1.69
BpP12	0.80 ns (86%)	1.75 ns (14%)	1.04	1.81
PhP12	0.75 ns (75%)	1.31 ns (25%)	1.05	1.73
BpP18	0.59 ns (58%)	0.96 ns (42%)	1.16	1.71
PhP18	0.70 ns (49%)	1.12 ns (51%)	1.14	1.80

[a] Results of biexponential decay analysis: $I(t) = B_1 \exp(t/\tau_1) + B_2 \exp(-t/\tau_2)$, $\varphi_i = B_i\tau_i/(B_1\tau_1 + B_2\tau_2)$. DW, Durbin–Watson parameter.

the fluorescence kinetics of some poly(aryleneethynylene)s in toluene and found deviations from first order decay. In some cases, a dependence of the weighted mean lifetimes emission on the recording wavelength was observed. **BpP18**, for example, is such a compound: $0.5 < \langle\tau\rangle < 0.6$ ns [10]. As noted by Bunz [1], poly(aryleneethynylene)s show lifetimes (which can be fitted to a single exponential) of approximately 0.5 ns, regardless of whether thiophene, benzene or pyridine units are separated by alkyne linkages. Our mean lifetimes, measured in dioxane, are somewhat larger (cf. Table I). In general, nonexponential fluorescence kinetics depending on the emission wavelength can be expected due to the distribution of polymer chain lengths, the distribution of conjugation lengths as well as energy migration processes along the polymer chains [18]. In the case of polyphenylenevinylenes (PPVs), effects which give rise to a transient bathochromic shift of the fluorescence spectra have also been studied using picosecond and femtosecond timeresolved methods and were interpreted by an energy dispersive hopping model [19].

We found a small variation of the decay kinetics curves over the emission spectral region for **BpP18** in dioxane. The time constants are larger, however, as compared to a toluene solution. The increase of the mean lifetime from the short wavelength wing (i.e., the spectral region of the related monomer emission) to the long wavelength edge of the spectrum excludes an explanation by a simple superposition of two independent decay processes originating from a monomer and a mono-exponential polymer kinetics for the polymers. The radiative fluorescence constants of the model compounds and the polymers are identical within the error limits, $k_f \approx (0.8 \pm 0.2)$ ns^{-1}; whereas the nonradiative deactivation rates differ appreciably: $k_{nr} \approx (0.05 \pm 0.05)$ ns^{-1} for the model compounds and $k_{nr} \approx (0.4 \pm 0.2)$ ns^{-1} for the polymers.

Tor et al. [13] found that the fluorescence maxima of 4,4′-substituted 3,8-bis-(phenylethynelene)-1,10-phenanthrolines depend strongly upon the solvent. We have also found a pronounced solvent dependence with our model compounds and polymers. As an example, the absorption and fluorescence spectra of **PhM12** and **PhP12** in different polar solvents are shown in Figs. 4a and b. In Fig. 5, the related Lippert plots are presented for the two model compounds. Due to the different dipole moments perpendicular to the long molecule axis of the phenanthroline (cisoid arrangment of the pyridine moieties) and the more stable transoid bipyridine units, a different solvation behavior might be expected. However, the phenanthroline and bipyridine model compounds show the same slopes thus indicating the dipole moment changes in S_0 and S_1 do not differ significantly. Surpris-
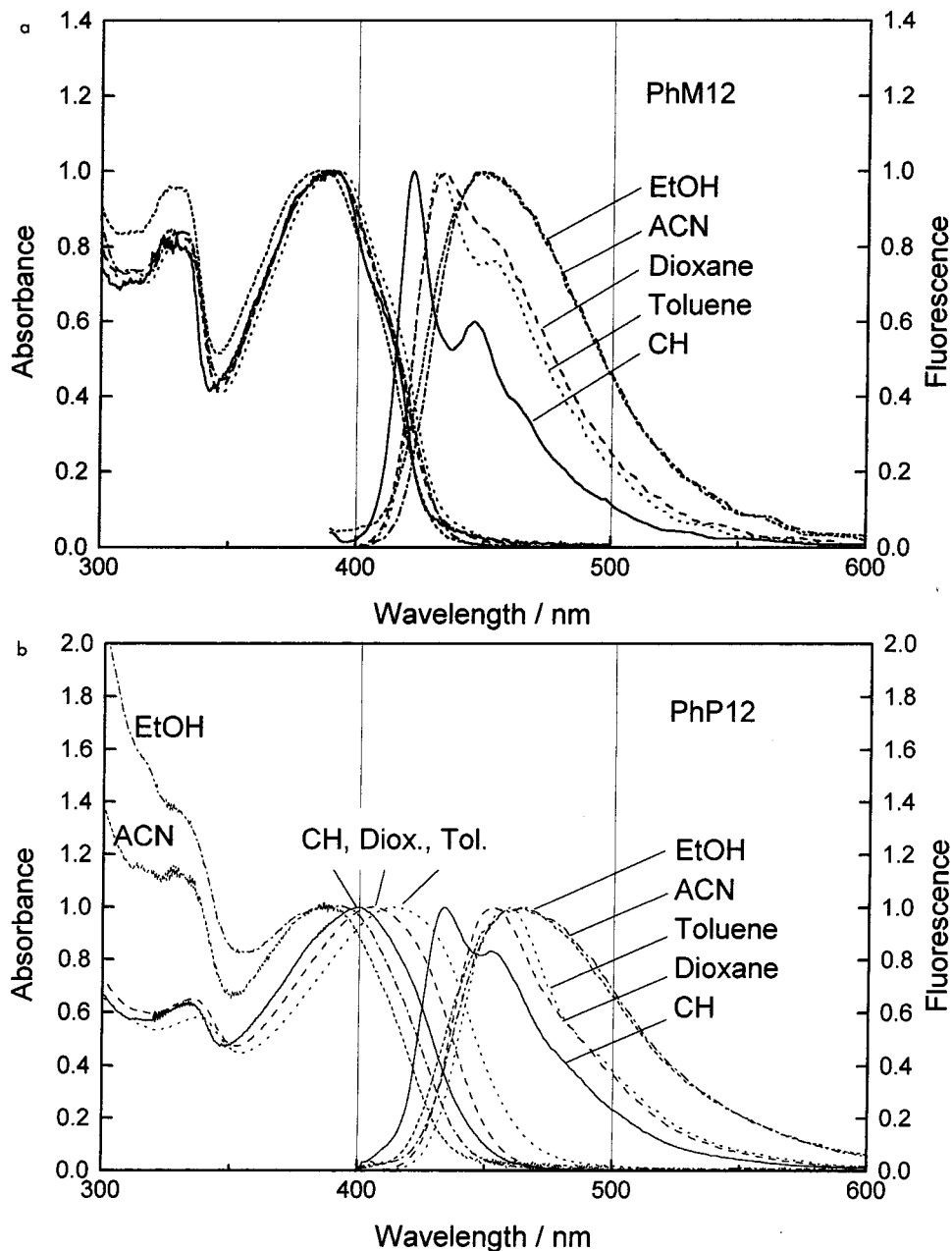
Fig. 4. Solvent dependence of absorption and fluorescence spectra at room temperature. (a) Monomer model compound **PhM12**; (b) polymer **PhP12**.

ingly, the slopes of the Lippert plots $\alpha \sim (\mu_1 - \mu_0)^2/a^3$ for the polymers are twice as large (**BpP18**: $\alpha = 7700\text{cm}^{-1}$, **PhP12**: $\alpha = 6700\text{cm}^{-1}$) as those measured for the monomer models (Fig. 5). The differences in the dipole moments $(\mu_1 - \mu_0)$ should therefore be larger for the polymers and/or the solvent cage radius should be smaller than for the model compounds. The assumption of a smaller solvent cage for the polymers, however, is proba-

bly unreasonable. The larger slope in the Lippert plot of the phenanthroline polymer **PhP12** is due to the stronger solvent dependence of the absorption spectra; cf Fig. 4b. These experimental findings obviously need more detailed investigation and discussion.

Luminescence investigations at low temperatures were performed on the model compounds **BpM18** and **PhM18** as well as on the polymers **BpP18** and **PhP18**
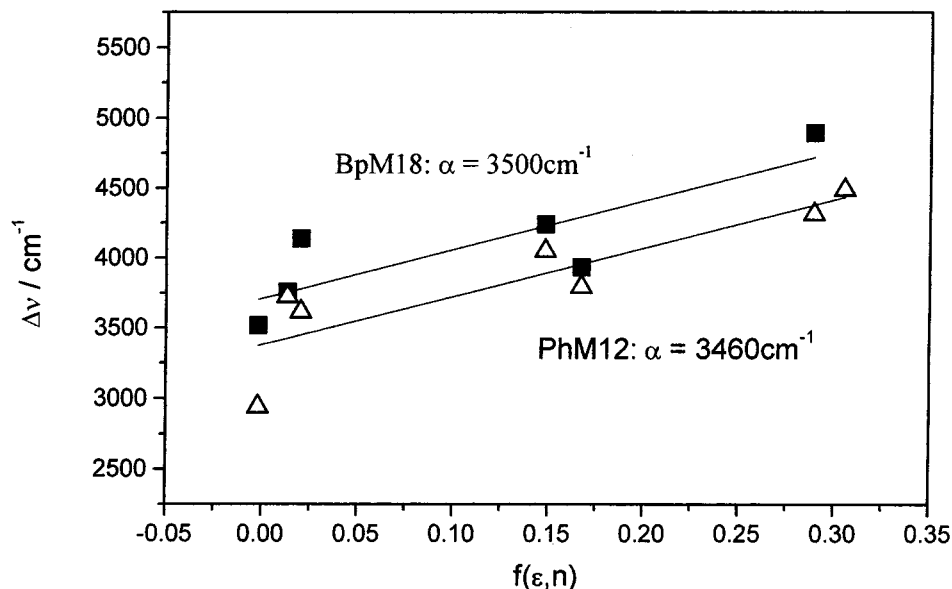
Fig. 5. Lippert plots $\Delta\nu = \alpha \times f(\varepsilon,n)$ of the monomer model compounds **BpM18** and **PhM12** with slopes α of 3500cm^{-1} and 3460cm^{-1}, respectively. $\Delta\nu = \nu_a - \nu_{f,cog}$, $\alpha = 2(\mu_1 - \mu_0)^2/hca^3$, $f(\varepsilon,n) = (\varepsilon - 1)/(2\varepsilon + 1) - (n^2 - 1)/(2\,n^2 + 1)$. cog, center of gravity; a, radius of the solvent cage.
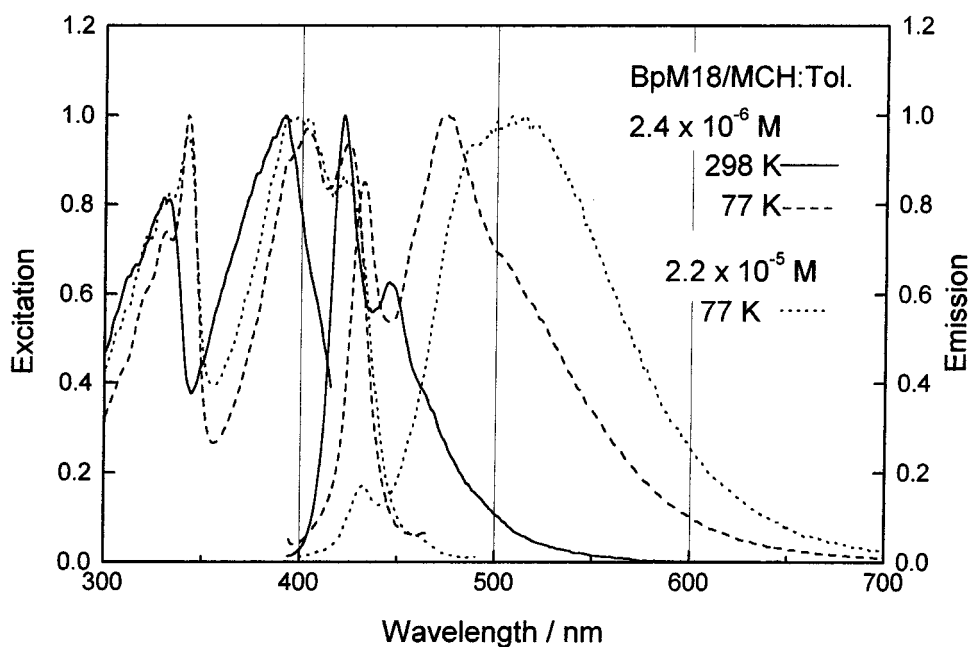

Fig. 6. Fluorescence excitation and emission spectra of a diluted (2.4 $\times$ 10^{-6} M) solution **BpM18** in MCH/Toluene 10:1 at room temperature and at 77 K and of a tenfold higher concentrated solution at 77 K.

in a methyl-cyclohexane (MCH)/toluene (10:1) mixture as well as in diethylether. Figure 6 shows the fluorescence and the fluorescence excitation spectra of **BpM18** dissolved in MCH/toluene at room temperature and at 77 K. Two concentrations differing by an order of magnitude were chosen. In comparison to the fluorescence spectrum at room temperature, the spectrum of the less concentrated solution shows a bathochromic shift as well as an increase in intensity at 500 nm. For the higher concentrated solution, the structured emission at 432 nm is observable only
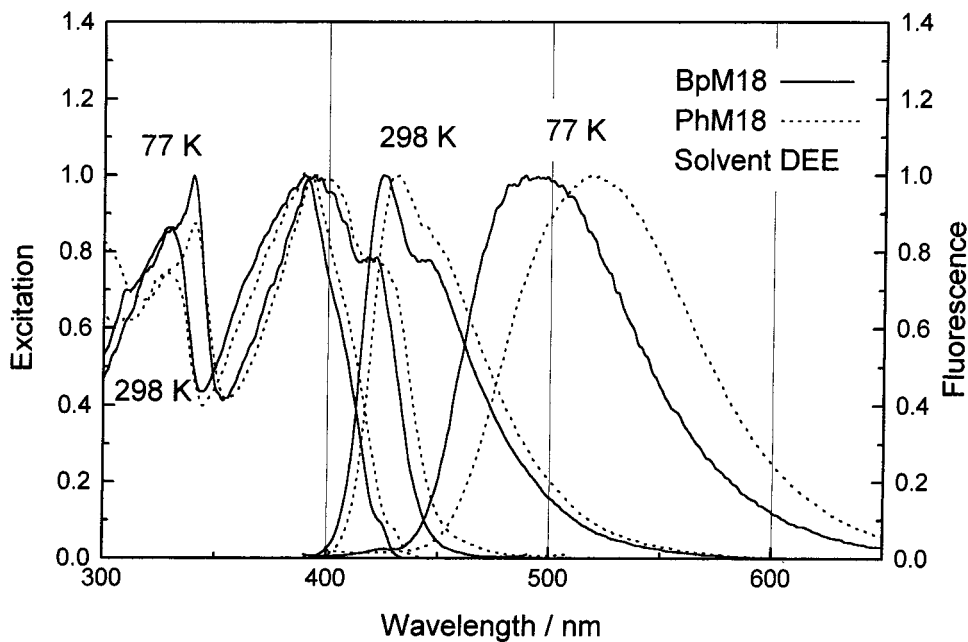
Fig. 7. Fluorescence excitation and emission spectra of diluted solutions of **BpM18** and **PhM18** in diethylether at room temperature and at 77 K.
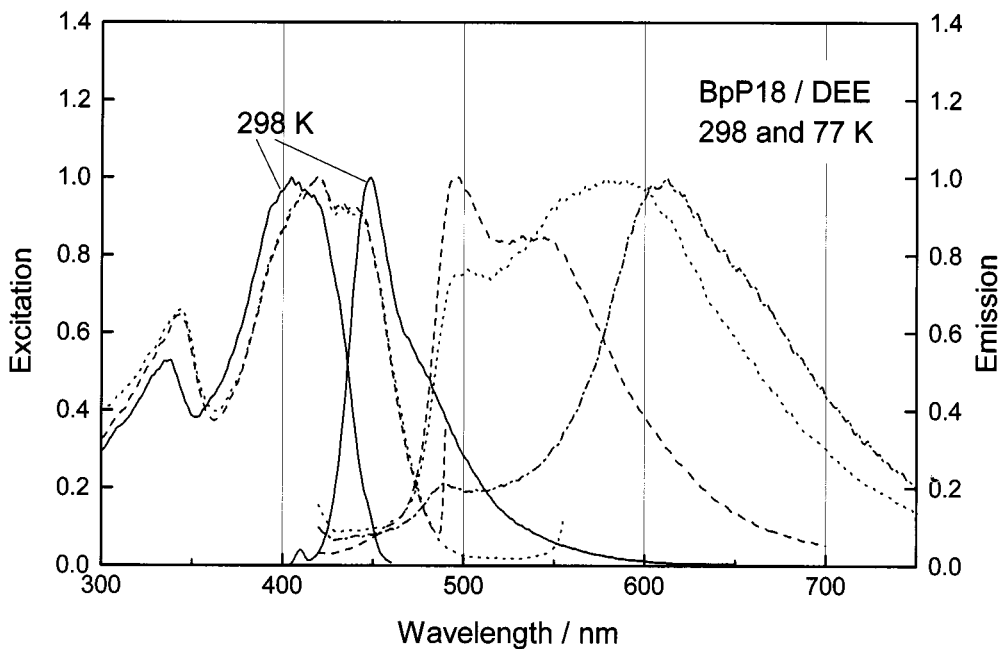

Fig. 8. Fluorescence excitation and emission spectra of diluted solutions of **BpP18** in diethylether at room temperature and at 77 K. The emission spectra at 77 K are measured with different frozen samples of the same solution.

as a pre-band to the broad and intense luminescence band at 500 nm. In contrast to this, the fluorescence excitation spectra depend only slightly upon the concentration of the sample and on the emission wavelength.

Comparable effects were found for **BpM18** and **PhM18** in diethylether; cf. Fig. 7. The transformation from the structured short-wavength emission to the broad unstructured one occurs in the temperature interval between 173 and 143 K as could be shown through systematic temperature variation. The transformation temperature lies considerably above the melting point of the solvent (133 K). The biexponential fit of the fluorescence decay of **BpM18** in diethylether at 77 K gave lifetimes of $\tau_1 = 3.5$ ns ($\varphi_1 = 0.29$) and $\tau_2 = 14.5$ ns ($\varphi_2 = 0.71$). These experimental findings point to an interpretation of the long-wavelength emission as an excimer fluorescence.

The situation is more complicated for the polymers. Figure 8 shows the fluorescence and the fluorescence excitation spectra of a 10^{-5} **M BpP18** solution in diethylether at room temperature and at 77 K. The spectra at 77 K were obtained from the same sample after repeated freeze-thaw cycles. In addition to the weak pre-band, we observed bands at 495 nm, 580 nm, and 610 nm. Interestingly enough, the intensity ratio of these bands differed from cycle to cycle. Obviously, aggregates of different sizes are present in the solid solution in addition to non aggregated polymer molecules in a non equilibrium distribution in solution. The relative amount of the different aggregates varies with an increasing number of freeze-thaw cycles to very slowly approach the thermodynamic equilibrium. Comparison of the fluorescence spectra of differently substituted poly(aryleneethynylene)s measured both in diluted CH_2Cl_2, solution and in films reported in ref. [20] support this interpretation. Poly(aryleneethynylene)s without bulky moieties in the polymer backbone show different fluorescence spectra in diluted solutions and in the film due to aggregate formation in the film. The incorporation of rigid three dimensional pentiptycene moieties into the conjugated polymer backbones prevent aggregation thus resulting in similar spectra for solutions and films [20].

CONCLUSIONS

Preventing the nearly free torsional motion around the carbon-carbon single bond connecting the pyridyl moieties in compounds containing bipyridine units by introducing an ethenylene bridge neither affects the spectral properties nor does it significantly change the deactivation behaviour. Since we recently succeeded in showing that the conjugation length in the polymers containing bipyridine is not larger than about two monomer units, we have to conclude from the unchanged spectral properties of the more stiff polymers that the conjugation length is not increased. Torsional motion around the carbon-carbon single bond cannot be the reason for the short conjugation length in the bipyridine containing polymers. When only the spectroscopic and the photophysical properties are of importance, replacing bipyridine by phenanthroline gives no advantages for application as luminescent polymers.

Luminescence investigations at low temperatures reveals a more complicated picture. The model compounds investigated show an excimer (or a preformed dimer or aggregate) fluorescence with a high quantum yield and an increased lifetime. Similar effects are observed for the polymers. The relative intensity of the fluorescence components which originate from single strand and variously aggregated polymers depends obviously on the temperature processing. Low temperature emission spectra recorded in highly viscous or solid solutions at comparatively low temperatures resemble the fluorescence spectra of solid films of the pure polymers at room temperature. Aggregation at low temperatures may possibly serve as a link between the fluorescence behaviour at room temperature in diluted solutions and the luminescence of solid films. A detailed study of the polymer film fluorescence is in progress. Intersystem crossing has been found to be insignificant. Only a weak long lived emission could be detected which is interpreted as phosphorescence.

ACKNOWLEDGMENTS

REFERENCES

1. U. H. F. Bunz (2000) *Chem Rev.* **100**, 1605–1644.
2. T. Yamamoto, W. Yamada, N. Tagaki, K. Kizu, T. Maruyama, N. Ooba, S. Tomaru, T. Kurihara, T. Kaino, and K. Kubota (1994) *Macromolecules* **27**, 6620–6626.
3. P. Wautelet, M. Moroni, L. Oswald, J. Le Moigne, A. Pham, J.-Y. Bigot, and S. Luzzati (1996) *Macromolecules* **29**, 446–455.
4. H. S. Nalwa (1997) in H. S. Nalwa (Ed.), *Handbook of Organic Conductive Molecules and Polymers*, *Vol. 4*, Wiley, Chichester, pp. 261–361.
5. G. Liu (1993) *Macromolecules* **26**, 5687–5962.
6. T. M. Swager, C. G. Gil, and M. S. Wrighton (1995) *J. Phys. Chem.* **99**, 4886–4893.

7. Q. Zhou and T.M. Swager (1995) *J. Am. Chem. Soc.* **117**, 12593–12602.

8. J. S. Schumm, D. L. Pearson, and J. M. Tour (1994) *Angew. Chem.* **106**, 1445–1448.

9. (a) K. D. Ley, C. E. Whittle, M. D. Bartberger, and K. S. Schanze (1997) *J. Am. Chem. Soc.* **119**, 3423–3424. (b) K. D. Ley and K. S. Schanze, *Coord. Chem. Rev.* (1998) **171**, 287–307.

10. U.-W. Grummt, E. Birckner, E. Klemm, D. A. M. Egbe, and B. Heise (2000) *J. Phys. Org. Chem.* **13**, 112–126.

11. A. Goeller and U.-W. Grummt (2000) *Chem. Phys. Lett.* **321**, 399–405.

12. M. Al-Higari, E. Birckner, B. Heise, and E. Klemm (1999) *J. Polym. Sci. A Polym. Chem.* **37**, 4442–4448.

13. H. S. Joshi, R. Jamshidi, and Y. Tor (1999) *Angew. Chem.* **111**, 2888–2891.

14. E. Birckner and U.-W. Grummt, unpublished results.

15. D. A. M. Egbe and E. Klemm (1998) *Macromol. Chem. Phys.* **100**, 2683–2688.

16. J. N. Demas and G. A. Crosby (1971) *J. Phys. Chem.* **75**, 991–1024.

17. H.-H. Perkampus, I. Sandeman, and C. J. Timmon (Eds.) (1998) *DMS UV Atlas Organischer Verbindungen*, Butterworths/Verlag Chemie, London, Vol. IV, H20/2.

18. B. Mollay and H. F. Kauffmann (1994) in R. Richard and A. Blumen (Eds.), *Disorder Effects on Relaxational Processes*, Springer Verlag Berlin, 1994, pp. 509–540.

19. K. Brunner, A. Tortschanoff, Ch. Warmuth, H. Bässler, and H. F. Kauffmann (2000) *J. Phys. Chem. B* **104**, 3781–3790.

20. (a) J.-Sh. Yang and T. M. Swager (1998) *J. Am. Chem. Soc.* **120**, 5321–5322. (b) J.-S. Yang and T. M. Swager (1998) *J. Am. Chem. Soc.* **120**, 11864–11873.